

Peptide Targeting of Fluorescein-Based Sensors to Discrete Intracellular Locales

Robert J. Radford, Wen Chyan, and Stephen J. Lippard*

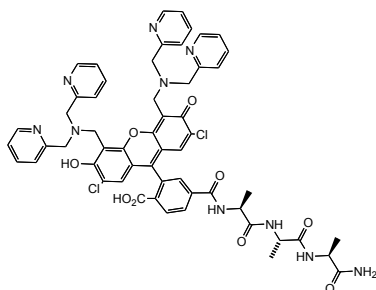
Department of Chemistry, Massachusetts Institute of Technology, 77 Massachusetts Avenue,
Cambridge, MA 02139; e-mail: lippard@mit.edu

Materials. HPLC grade acetonitrile, anhydrous *N,N*-dimethylformamide (DMF), dichloromethane, 4-methylpiperidine, *N,N*-diisopropylethylamine (DIPEA), potassium hydroxide, TraceSELECT nitric acid ($\geq 69.0\%$), Fmoc-Ala-OH, porcine liver esterase, and all metal salts were purchased from Sigma-Aldrich. 2-(7-Aza-1*H*-benzotriazole-1-yl)-1,1,3,3-tetramethyluronium hexafluorophosphate (HATU) and *O*-benzotriazole-*N,N,N',N'*-tetramethyluronium hexafluorophosphate (HBTU) were procured from Oakwood Chemicals. Fmoc-Lys(MTT)-OH and Fmoc-Cha-OH (Fmoc-F_x-OH) were obtained from Aapptec. MitoTracker Red FM, Hoechst 33258 stain, Dextran Red, and LysoTracker Red DND-99 were purchased from Life Technologies. All solvents were ACS reagent grade and commercially available reagents were used as received. 2',7'-Dichloro-5-carboxyfluorescein diacetate and 6-CO₂H Zinpyr-1 were prepared according to literature procedures.¹ An Agilent Technologies 1200 series HPLC system equipped with a multi-wavelength detector, automated injector, and thermostated fraction collector was used to purify all constructs. The purity of each peptide was assessed by analytical HPLC on a similar instrument. Mass spectra (ESI-MS) were collected on an 1100 series Agilent LC/MSD ion trap with a mobile phase composed of methanol, water, and formic acid (49.95, 49.95, 0.1%, v/v) or submitted for MALDI-MS at MIT's Koch Institute for Integrative Cancer Research. Aqueous solutions were prepared using deionized water from a Millipore purification system (resistivity = 18.2 MΩ cm). Molecular biology grade piperazine-*N,N'*-bis(2-ethanesulfonic acid) (PIPES) and 99.999% KCl were purchased from Aldrich. In order to remove adventitious metal ions, buffered solutions were treated with Chelex resin (Bio-Rad) according to manufacturer specifications. A 50 mM zinc(II) stock solution was prepared using 99.999% anhydrous ZnCl₂ (Aldrich). Stock solutions for metal ion selectivity tests were prepared using 99.9% anhydrous MgCl₂ (Aldrich), 99.99% anhydrous MnCl₂ (Alfa Aesar), 99.5% anhydrous CoCl₂ (Sigma-Aldrich), 98% NiCl₂ · 6 H₂O (Aldrich), 98% CuCl₂ · 6 H₂O (Alfa Aesar), 99.9% anhydrous CaCl₂ (Aldrich), and 99.999% anhydrous CdCl₂ (Aldrich). UV-vis spectra were recorded on a Varian Cary 50 Bio UV-visible spectrophotometer. Fluorescence spectra were recorded on a Quanta Master 4 L-format scanning spectrofluorimeter (Photon Technology International). The acquisition temperature was kept constant by circulating water bath. Sample solutions were placed in quartz cuvettes (Starna) with 1 cm path lengths. Stock solutions of all peptides were prepared in spectroscopic grade DMSO, portioned in 50 μL aliquots, and stored in the dark at -40 °C.

Peptide Synthesis. Solid-phase peptide synthesis was carried out using an Aapptec Focus Xi automated peptide synthesizer. Fmoc groups were removed by treating the resin with a solution of 20% (v/v) 4-methylpiperidine in DMF for 2 × 10 min periods. For typical coupling reactions, 4 equiv of an Fmoc-protected amino acid were combined as a solid with 4 equiv of solid HBTU. Immediately prior to the coupling reaction, the mixture was dissolved in a freshly prepared solution of 10% (v/v) DIPEA in anhydrous DMF. The resin was allowed to react in the coupling solution for 30 min. Manual couplings were performed using previously reported methods.² Unless otherwise noted, all peptides were cleaved by treatment with a TFA cocktail (1.5 mL) consisting of TFA, triisopropylsilane, and water (95, 2.5, 2.5%, v/v) for 2 hours. All peptides

were purified by HPLC using a Zorbax C18 semi-preparative column (9.5 × 250 mm) at a flow rate of 3 mL min⁻¹. HPLC purification was carried out using a two-solvent system: A = 0.1% (v/v) TFA in water; B = 0.1% (v/v) TFA in acetonitrile. The purity of each construct was assessed using a Zorbax C18 analytical column (4.6 mm × 250 mm) at a flow rate of 1 mL min⁻¹, using the same water/acetonitrile solvent system. Unless otherwise noted, the identity of each peptide was verified using ESI-MS.

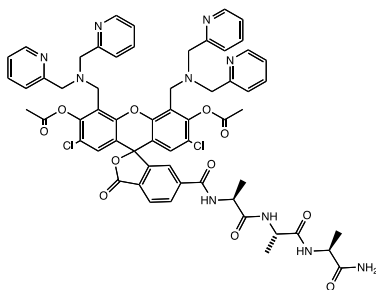
ZP1-A₃



ZP1-A₃ was synthesized on the 30-μmol scale using Rink amide resin. After addition of 6-CO₂H ZP1 to the N-terminus of the resin-bound peptide, approximately 10 mg of the resin was removed and cleaved. The crude mixture of ZP1-A₃ was diluted with 10 mL of water and lyophilized to yield an orange film. The film was dissolved in water with 0.1% (v/v) TFA in water and purified by HPLC according to the following protocol: isocratic flow, 0-3 min, 5% B; linear gradient 1, 3-5 min, 5-20% B; linear gradient 2, 5-35 min, 20-35%B. Equivalent fractions from

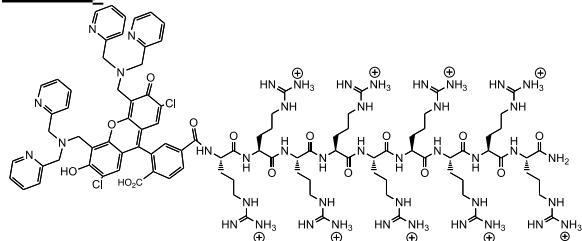
successive runs were pooled and lyophilized. The purity of ZP1-A₃ was assessed by analytical HPLC (Figure S19) according to the following protocol: isocratic flow, 0-5 min, 10% B, linear gradient 1, 5-35 min, 10-50% B. Retention time = 17.4 min; ZP1-A₃ was determined to be ≥98% pure based on the integrated absorbance signal at 220, 250, and 520 nm, respectively. The identity of ZP1-A₃ was confirmed by ESI-MS (positive mode); chemical formula: C₅₆H₅₂Cl₂N₁₀O₉; *m/z* calcd for [M+H]⁺ = 1079.3, found: 1079.3; *m/z* calcd for [M+2H]²⁺ = 540.15, found: 540.1.

DA-ZP1-A₃

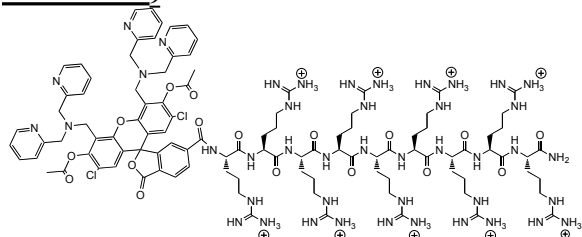


The remaining ~40 mg from the synthesis of ZP1-A₃ was placed in a solution of acetic anhydride (50%, v/v) in DMF for 5 h. The resin was subsequently washed, dried, and cleaved using standard SPPS protocols (vide supra). Using analytical HPLC, we estimated the yield for the acetylation reaction to be 44%. DA-ZP1-A₃ was purified by HPLC using the same protocol listed for ZP1-A₃. Equivalent fractions from successive HPLC runs were pooled and lyophilized. The purity of DA-ZP1-A₃ was determined to be ≥99% pure by analytical HPLC (Figure S20)

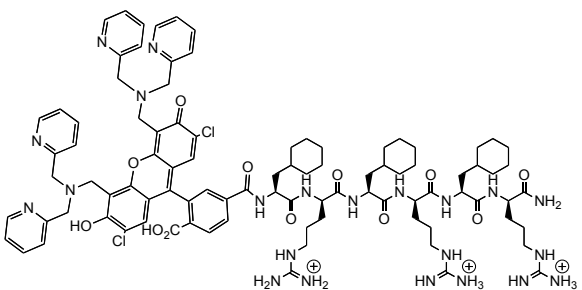
using the protocol listed for ZP1-A₃. Retention time = 24.71 min. The identity of DA-ZP1-A₃ was confirmed by ESI-MS (positive mode); chemical formula: C₆₀H₅₆Cl₂N₁₀O₁₁; *m/z* calcd for [M+Na]⁺ = 1184.3, found: 1185.4; *m/z* calcd for [M+H]⁺ = 1163.4, found: 1163.4; *m/z* calcd for [M+2H]²⁺ = 582.2, found: 583.1

ZP1-R₉

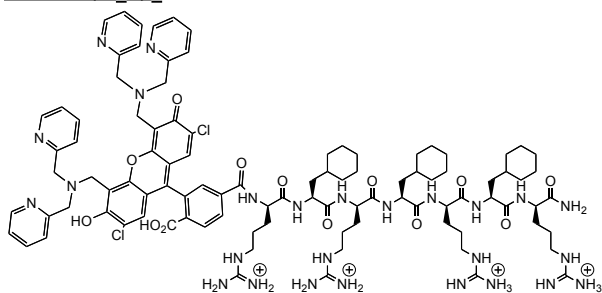
(Figure S21), using the same gradient. Retention time = 15.87 min. The identity of ZP1-R₉ was confirmed by ESI-MS (positive mode); chemical formula: [C₁₀₁H₁₅₄Cl₂N₄₃O₁₅]⁹⁺; *m/z* calcd for [M]²⁺ = 1139.6, found: 1137.3; *m/z* calcd for [M]³⁺ = 759.7, found: 758.4; *m/z* calcd for [M]⁴⁺ = 569.8, found: 569.1.

DA-ZP1-R₉

A 3 mL portion of a 50% (v/v) solution of acetic anhydride in DMF was added to 300 μL of a 3.2 mM solution of ZP1-R₉ in DMSO. The mixture was allowed to react in the dark for 8 h, after which it was diluted with 5 mL of water and lyophilized. The crude lyophilized solid was purified by HPLC using the same conditions reported for ZP1-R₉. The yield of the reaction was estimated by analytical HPLC to be 92% based on the integrated absorbance signal at 220 nm. Fractions from successive HPLC runs were pooled and lyophilized. DA-ZP1-R₉ was determined to be ≥99% pure by analytical HPLC (Figure S22). Retention time = 21.2 min. The identity of DA-ZP1-R₉ was confirmed by MALDI-MS; chemical formula: C₁₀₅H₁₄₉Cl₂N₄₃O₁₇; *m/z* calcd for [M+H]⁺ = 2355.16, found: 2356.8.

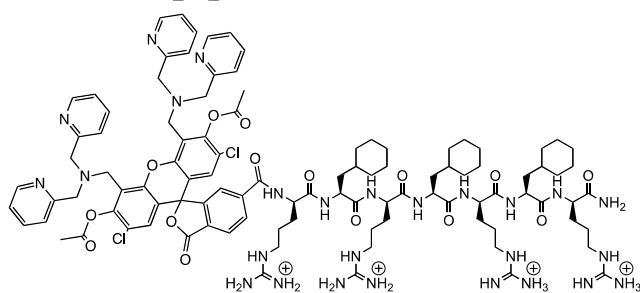
ZP1-(F_xr)₃

ZP1-(F_xr)₃ was synthesized on the 15 μmol scale using Rink amide resin. ZP1-(F_xr)₃ was purified by HPLC using matched Vydac C18 semi-prep (9.5 × 250 mm) and analytical (5 μm, 4.6 × 250 mm) columns according to the following protocol: isocratic flow, 0-5 min, 10% B, linear gradient 1, 5-35 min, 10-50% B. ZP1-(F_xr)₃ was determined to be 95.2 % pure by analytical HPLC (Figure S23). Retention time = 28.1 min. The identity of ZP1-(F_xr)₃ was confirmed by ESI-MS; chemical formula [C₉₂H₁₂₁Cl₂N₂₂O₁₂]³⁺; *m/z* calcd for [M]⁺ = 1795.89, found: 1796.0; *m/z* calcd [M]²⁺ = 897.94, found: 898.5.

ZP1-r(F_xr)₃

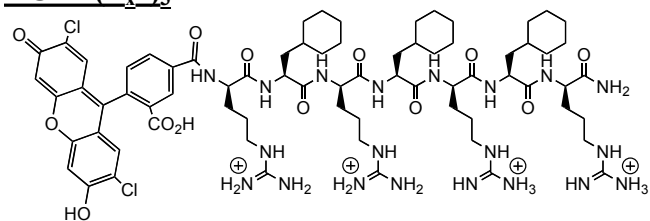
ZP1-r(F_xr)₃ was synthesized on the 30- μ mol scale using a Rink amide resin using the same method as all other peptides, except that only 2 equiv of 6-CO₂H ZP1 (55 mg) were used instead of the usual 4; this change did not appear to affect the coupling yield in any significant way. ZP1-r(F_xr)₃ was purified by HPLC according to the following protocol: isocratic flow, 0-5 min, 10% B, linear gradient

1, 5-35 min, 10-50% B. Fractions from successive HPLC runs were pooled and lyophilized. ZP1-r(F_xr)₃ was determined to be $\geq 98\%$ pure by analytical HPLC (Figure S24). Retention time = 23.3 min. The identity of ZP1-r(F_xr)₃ was confirmed by ESI-MS; chemical formula: [C₉₈H₁₃₄Cl₂N₂₆O₁₃]⁴⁺; *m/z* calcd for [M]²⁺ = 976.5, found: 976.5; *m/z* calcd for [M]³⁺ = 651.0, found: 651.3.

DA-ZP1-r(F_xr)₃

A 1 mL portion of acetic anhydride was added to a 100 μ L of a 2.1 mM solution of ZP1-r(F_xr)₃ in DMSO and the mixture was allowed to react in the dark for 4 hours. The reaction mixture was diluted to 5 mL total volume with water and lyophilized. The crude mixture was purified by HPLC using the same gradient reported for ZP1-r(F_xr)₃.

The yield for the acetylation reaction was estimated by HPLC to be 52% based on the integrated absorbance at 220 nm. DA-ZP1-r(F_xr)₃ was determined to be $\geq 99\%$ pure by analytical HPLC (Figure S25). Retention time = 26.8 min. The identity of DA-ZP1-r(F_xr)₃ was confirmed by ESI-MS; chemical formula: [C₁₀₂H₁₃₈Cl₂N₂₆O₁₅]⁴⁺; *m/z* calcd for [M]²⁺ = 1018.5, found: 1018.5, *m/z* calcd for [M]³⁺ = 679.0, found: 679.3; *m/z* calcd for [M]⁴⁺ = 509.25, found: 509.8.

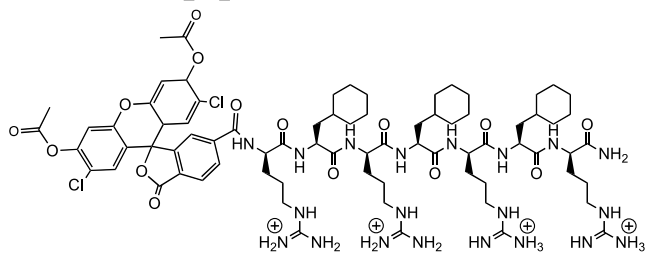
DCF-r(F_xr)₃

DCF-r(F_xr)₃ was synthesized on the 30- μ mol scale using Rink amide resin. After the synthesis of the peptide scaffold was complete, we attempted to couple 2',7'-dichloro-5-carboxyfluorescein diacetate (DA-DCF) to the N-terminus of the peptide.

But, using a combination of analytical HPLC and ESI-MS, it was determined that the acetyl protecting groups were removed during either the coupling or cleavage step. The resin was treated with the TFA cocktail and the resulting peptide, DCF-r(F_xr)₃, was purified by HPLC. DCF-r(F_xr)₃ was determined to be $\geq 95\%$ pure by analytical HPLC (Figure S26). Retention time = 28.7 min. The identity of DCF-r(F_xr)₃ was confirmed by ESI-MS; chemical formula:

$[C_{72}H_{108}Cl_2N_{20}O_{13}]^{4+}$; m/z calcd for $[M]^{2+} = 765.4$, found: 765.3, m/z calcd for $[M]^{3+} = 510.3$, found: 510.0; m/z calcd for $[M]^{4+} = 382.7$, found: 383.0.

DA-DCF-r(F_xr)₃



A 300 μ L portion of acetic anhydride was added to a 75 μ L of a 4.8 mM solution of DCF-r(F_xr)₃ in DMSO and the reaction was stirred in the dark for 4 h. The reaction was worked-up as described above. DA-DCF-r(F_xr)₃ was determined to be $\geq 95\%$ pure by analytical HPLC (Figure S27). Retention time = 34.02 min. The identity of DA-DCF-r(F_xr)₃ was confirmed by ESI-MS; chemical formula: $[C_{76}H_{114}Cl_2N_{20}O_{15}]^{4+}$; m/z calcd for $[M]^{2+} = 808.1$, found: 806.3, m/z calcd for $[M]^{3+} = 538.7$, found: 538.0.

Photophysical and Zinc-Binding Properties of Peptide Constructs

General. Spectroscopic measurements for all peptides were carried out in aqueous buffer (50 mM PIPES, 100 mM KCl; pH 7). All buffers were treated with Chelex100 resin (BioRad) according to manufacturer's specification. Except where noted, all fluorescence data were obtained by exciting at 495 nm and recording the emission between 500-650 nm, with a 0.1 sec integration time. Emission spectra represent the average of three scans. The quantum yields were determined by referencing peptide solutions to fluorescein ($\lambda_{ex} = 495$ nm; $\Phi = 0.95$) in 0.1 M NaOH_(aq).³

In vitro Assessment of Zinc Response. A 2 mL solution of ca. 1 μ M peptide in buffer at 25 °C was prepared and the fluorescence spectrum acquired. A 2- μ L aliquot of 50 mM ZnCl₂ in water was then added and the fluorescence spectrum was measured. Lastly, a 2- μ L aliquot of 100 mM EDTA_(aq) (pH 7) was added, the system was allowed to equilibrate (~30 min), after which the fluorescence spectrum was again measured. Data were normalized to the fluorescence signal at the emission maximum ($\lambda_{em} = 533$ nm). The zinc-induced fluorescence response for DA-ZP1-R₉ and DA-ZP1-r(F_xr)₃ is given in Figure S4. The fluorescence response of DA-ZP1-A₃ can be found in the main text Figure 2b.

Apparent K_{d-Zn} for Peptide Constructs. Apparent zinc-binding affinities (K_{d-Zn}) were determined in buffer using either 1 mM EGTA or 1 mM CaEDTA as competing ligands. Aliquots of ZnCl₂ were successively added, and the emission spectra were recorded once equilibrium had been established (30-60 min when using CaEDTA; ca. 3 min when using EGTA). For a given concentration of total zinc, the concentration of free zinc ions buffered in solution was calculated using the MaxChelator program (<http://maxchelator.stanford.edu/>). The resulting binding isotherms were fit according to single site model using Dynafit (Biokin). Representative binding isotherms are shown in Figures S5 and 6.

pH-Dependent Fluorescence Titrations. A 5 mL portion of a 1- μ M solution of ZP1-A₃ or DA-ZP1-A₃ was prepared in buffer (17.5 mM sodium acetate, 100 mM KCl, 0.25 mM EDTA, pH 3.5) The pH of the solution was increased from 3.5 to 8.5 by successive addition of KOH_{aq}. Total

amount of KOH_{aq} was kept below 5% of the total volume. At a given pH value, the integrated fluorescence intensity was calculated for the average of three scans.

Metal Ion Selectivity. The metal ion selectivity of ZP1-A₃ and DA-ZP1-A₃ was assessed by using a modified literature procedure.⁴ The fluorescence spectrum of a 2-mL solution of peptide (ca. 1 μM) in buffer was acquired before and after addition of a 2- μL aliquot of a given metal(II) salt stock solution (0.8 M CaCl_2 or MgCl_2 ; 20 mM MnSO_4 , CoCl_2 , NiCl_2 , CuCl_2 or CdCl_2). Next, a 2- μL aliquot of ZnSO_4 (10 mM) was added and the fluorescence spectrum was measured. Fluorescence signals were integrated and normalized to the integrated signal the appropriate metal-free peptide construct.

Kinetics of Zinc-Mediated Deacetylation. A stirred solution of DA-ZP1-A₃ (5.5 μM), DA-ZP1-R₉ (2 μM), or DA-ZP1-r(F_xr)₃ (1 μM) in buffer was equilibrated and maintained at 37 °C. The hydrolysis of the acetyl groups on DA-ZP1-peptide was monitored by measuring the increase in absorbance at 520 nm in the presence of EDTA (100 μM) or at 510 nm in the presence of ZnCl_2 (100 μM). Data were normalized and fit to a single exponential function using Igor Pro software. Representative traces for each construct can be found in Figure S7; calculated k_{obs} are listed in Table S2.

Mammalian Cell Culture, Labeling, and Imaging Procedures

General. HeLa cells were cultured at 37 °C under a humidified atmosphere of 5% CO_2 in high glucose Dulbecco's Modified Eagle Medium (High Glucose DMEM, Life Technologies) supplemented with 10% (v/v) fetal bovine serum (FBS, HyClone), penicillin (100 $\mu\text{g mL}^{-1}$), and streptomycin (100 $\mu\text{g mL}^{-1}$). For live cell imaging, cells were seeded in 35-mm poly-D-Lys coated glass-bottom culture dishes (MatTek Corporation) 24 to 48 h before imaging. For all imaging experiments involving addition of sensors and fluorophores dissolved in DMSO, the DMSO was kept below 1% (v/v).

Fluorescence Microscopy. Imaging experiments were performed using a Zeiss Axiovert 200M inverted epifluorescence microscope equipped with an EM-CCD digital camera (Hamamatsu) and a MS200 XY Piezo Z stage (Applied Scientific Instruments). The light source was an X-Cite 120 metal-halide lamp (EXFO). Fluorescence images were obtained using an oil-immersion objective at 63 \times magnification. The microscope was operated using Volocity software (Perkin-Elmer).

Imaging Peptide Constructs in Live HeLa Cells. The localization of fluorophore-labeled peptides in HeLa cells was investigated by pretreating cells with dye- and serum-free medium supplemented with a given construct and an organelle specific dye for 30 min prior to imaging. The plates were then washed with 2 \times 1 mL dye- and serum-free DMEM, bathed in 2 mL of medium containing 25 μM ZnPT, and imaged by multichannel fluorescence microscopy.

Quantifying Intracellular Zinc Response. To prepare the zinc-enriched medium, stock solutions of aqueous ZnCl_2 and sodium pyrithione in DMSO were premixed and diluted to a final concentration of 25 μM with dye- and serum-free DMEM. After initial images were acquired, medium in the imaging dish was replaced with zinc-enriched medium. The cells were

allowed to equilibrate (~ 10 min) and then the image acquisition process was repeated. The zinc-enriched medium was again exchanged on stage for dye- and serum-free DMEM containing 50 μ M *N,N,N',N'*-tetrakis-(2-pyridylmethyl)ethylenediamine (TPEN). After a 10 min equilibration period, the final set of images were acquired. A minimum of three plates representing at least two passage numbers was tested. For each plate, images were acquired from at least three regions of interest. Data were normalized to the average fluorescence signal for the initial images, which was set to unity. All settings (i.e. exposure time, sensitivity, contrast) were kept constant for each image series. Images were processed with ImageJ.

Co-localization Analysis of Peptide Constructs with Organelle-Specific Dyes. To calculate Pearson's *r* values, images were first deconvoluted using a calculated point-spread function (PSF) map based on emission wavelength, refractive index of the medium ($n = 1.518$), and the numerical aperture (1.4). Deconvoluted channels (i.e. sensor and organelle trackers) were merged and analyzed using an ImageJ plugin as previously described.⁵ The analysis area covered the entire cell body. The minimum threshold was set to the background intensity for the image. This process was repeated for all cells in the region-of-interest and for each set of images, which spanned several plates and represented multiple cell passages.

Table S1. Photophysical and zinc-binding properties of various Zinpyr constructs.

Construct	λ_{abs} (nm), $\epsilon \times 10^4$ (M ⁻¹ cm ⁻¹)		λ_{em} (nm), Φ		K_d (nM) ^b
	Apo	+Zn	Apo	+Zn	
ZP1 ^a	515, 7.9	507, 8.4	531, 0.38	527, 0.87	0.7 \pm 0.1
(6-CO ₂ Et) ZP1 ^a	519, 6.1	509, 7.2	531, 0.13	528, 0.67	0.37 \pm 0.04
ZP1-A ₃	519, 8.7 \pm 0.5	509, 9.7 \pm 0.5	533, 0.14 \pm 0.01	529, 0.75 \pm 0.03	0.38 \pm 0.04
DA-ZP1-A ₃	–	509	–	530, 0.80 \pm 0.03	n.d.
ZP1-R ₉	525, 8.3 \pm 0.3	511, 8.6 \pm 0.2	533, 0.13 \pm 0.01	531, 0.73 \pm 0.01	0.36 \pm 0.04
DA-ZP1-R ₉	–	511	–	530, 0.74 \pm 0.01	n.d.
ZP1-(F _x r) ₃	521, 6.1	510, 4.8	534, 0.13 \pm 0.013	529, 0.71 \pm 0.062	0.68 \pm 0.04
ZP1-r(F _x r) ₃	525, 8.2 \pm 0.7	512, 8.7 \pm 0.9	535, 0.07 \pm 0.02	532, 0.73 \pm 0.02	1.2 \pm 0.2
DA-ZP1-r(F _x r) ₃	–	511	–	530, 0.79 \pm 0.05	n.d.

All measurements were made in buffer (50 mM PIPES and 100 mM KCl; pH 7). ^aData taken from ref. (6).

^bApparent dissociation constants (K_{d-Zn}) were measured in the presence of either 1 mM EGTA or 1 mM EDTA, 2 mM CaCl₂ as competing ligands (vide supra). n.d. = not determined.

Table S2. Observed rate constants (k_{obs}) for zinc binding to DA-ZP1-peptide constructs.

Construct	+ZnCl ₂		+EDTA	
	k_{obs} (min ⁻¹)	$t_{1/2}$ (min)	k_{obs} (min ⁻¹)	$t_{1/2}$ (min)
DA-ZP1-A ₃	13.1 ± 0.2	0.0528 ± 8.4×10 ⁻⁴	2.38×10 ⁻³ ± 7.6×10 ⁻⁶	290 ± 1
DA-ZP1-R ₉	12.0 ± 1.4	0.058 ± 0.006	2.92×10 ⁻³ ± 8.14×10 ⁻⁵	236 ± 6.6
DA-ZP1-r(F _x r) ₃	5.75 ± 1.16	0.12 ± 0.02	2.64×10 ⁻³ ± 1.9×10 ⁻⁴	263 ± 18

Observed rate constants (k_{obs}) were calculated by fitting the change in the absorption band associated with ZP1 ($\lambda = 510$ nm (zinc bound) or $\lambda = 520$ nm (metal free)) to a single exponential function using Igor Pro. Reported values are the average of at least three trials. Representative kinetic traces are given in Figure S7.

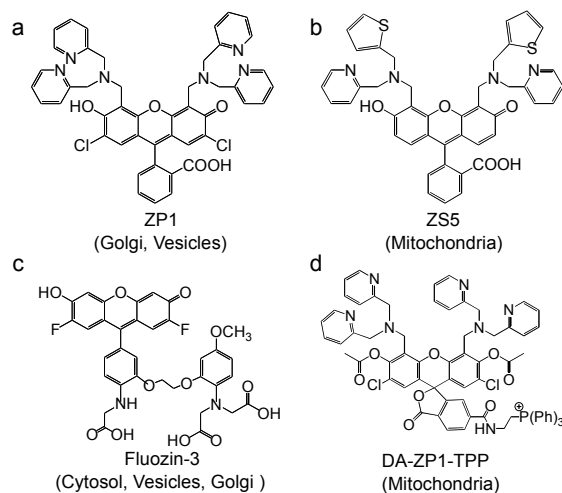


Figure S1. Line drawings of representative fluorescein-based mobile zinc sensors. The reported cellular localization of each probe is given in parentheses.

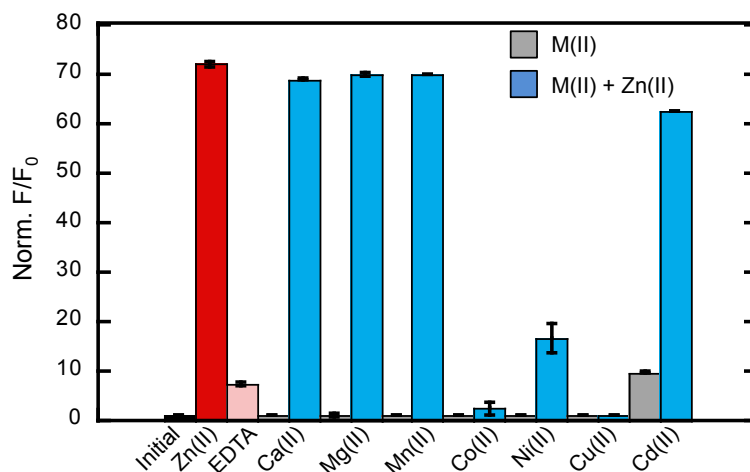


Figure S2. The fluorescence response of DA-ZP1-A₃ is selective for Zn(II) over other M(II) salts. Solutions were prepared containing 0.5 μ M DA-ZP1-A₃ in buffer (50 mM PIPES, 100 mM KCl; pH 7). Fluorescence spectra were acquired initially (Initial), in the presence of 10 μ M ZnCl₂ (Zn(II)), and then again in the presence of 20 μ M EDTA (EDTA). The process was repeated for each M(II) salt. Grey bars represent the normalized integrated fluorescence intensity of DA-ZP1-A₃ after addition of 10 μ M (MnCl₂, CoCl₂, NiCl₂, CuCl₂, or CdCl₂) or 400 μ M (CaCl₂ or MgCl₂) metal salt. Blue bars correspond to the normalized integrated fluorescence intensity of DA-ZP1-A₃ after addition of 10 μ M ZnCl₂ to the solution containing the indicated M(II) salt. Data were normalized to the initial integrated fluorescence intensity of DA-ZP1-A₃, which was set to unity.

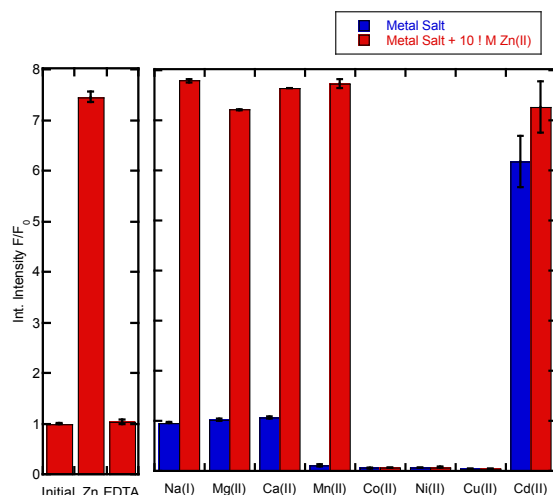


Figure S3. The fluorescence response of ZP1-A₃ is selective for Zn(II) over other M(II) salts. A solution was prepared containing 0.5 μ M ZP1-A₃ in buffer (50 mM PIPES, 100 mM KCl; pH 7). Fluorescence spectra were acquired initially (Initial), in the presence of 10 μ M ZnCl₂ (Zn), and then again in the presence of 20 μ M EDTA (EDTA). The process was repeated for each M(II) salt. Blue bars represent the normalized integrated fluorescence intensity of ZP1-A₃ after addition of 10 μ M (MnCl₂, CoCl₂, NiCl₂, CuCl₂, or CdCl₂) or 400 μ M (CaCl₂ or MgCl₂). Red bars correspond to the normalized integrated fluorescence intensity of ZP1-A₃ after addition of 10 μ M ZnCl₂ to the solution containing the indicated M(II) salt. Data were normalized to the initial integrated fluorescence intensity of ZP1-A₃, which was set to unity.

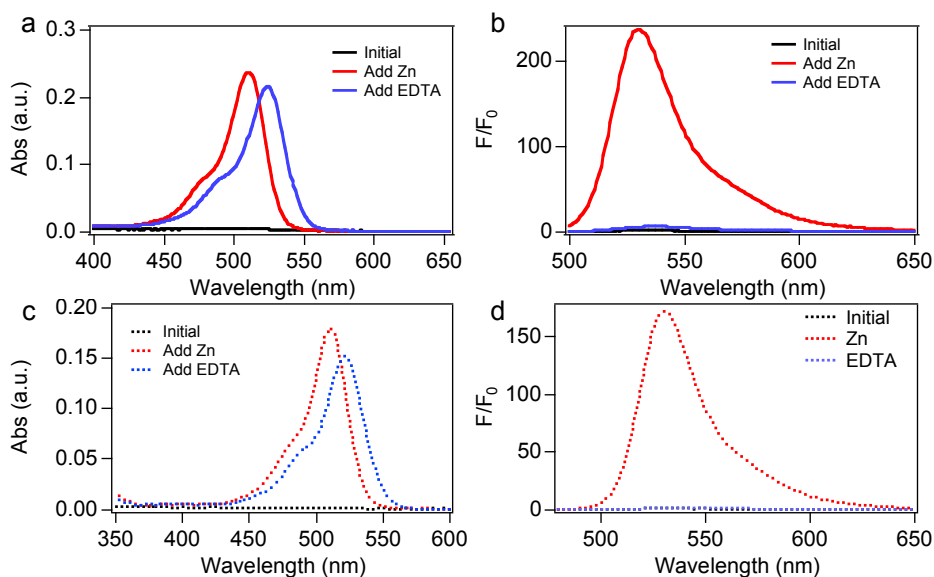


Figure S4. (a) Absorbance and (b) fluorescence spectra of a 2.5 μ M solution of DA-ZP1-R₉ in buffer initially (black line), upon addition of 100 μ M ZnCl₂ (red line), and after addition of 200 μ M EDTA (blue line). (c) Absorbance and (d) fluorescence spectra of a 1.8 μ M solution of DA-ZP1-r(F_xr)₃ in buffer initially (black, dotted line), upon addition of 100 μ M ZnCl₂ (red, dotted line), and after addition of 200 μ M EDTA (blue, dotted line).

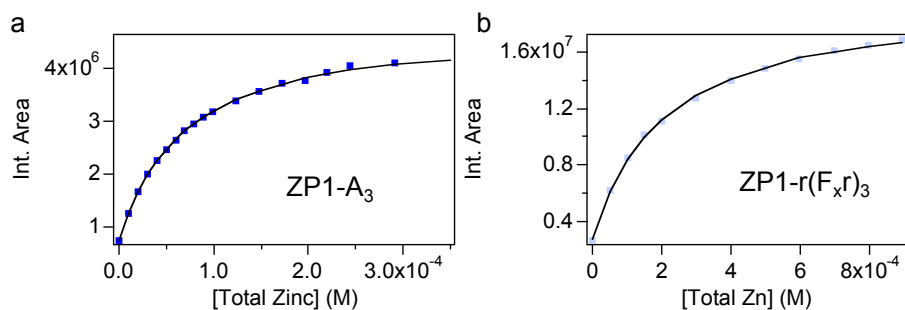


Figure S5. Representative zinc-binding isotherms (squares) and fits (lines) for (a) ZP1-A₃, (b) ZP1-r(F_xr)₃. Titrations were carried out in buffer (50 mM PIPES, 100 mM KCl, 1 mM EGTA; pH 7) using EGTA as a competing ligand. Successive aliquots of a 100 mM ZnSO₄ stock solution increased the total concentration of zinc in solution. The volume of zinc added never exceeded 5% of the total volume. Isotherms were fit in Dynafit (Biokin) using an apparent zinc dissociation constant for EGTA of $K_{d-Zn} = 6.367 \times 10^{-9}$ M. The EGTA K_{d-Zn} was calculated using the maxchelator program; 25 °C, pH 7.0, $I = 0.1$ M.

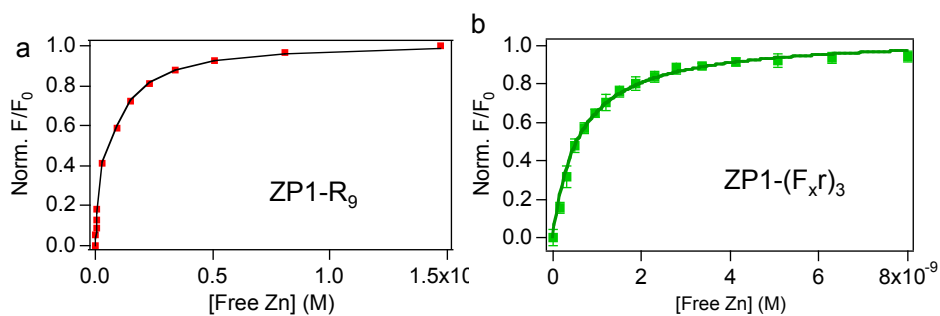


Figure S6. Representative zinc-binding isotherms (squares) and fits (lines) for (a) ZP1-R₉, (b) ZP1-(F_xr)₃. Titrations were carried out in buffer (50 mM PIPES, 100 mM KCl, 1 mM EDTA, 2 mM CaCl₂; pH 7) using CaEDTA as a competing ligand. Successive aliquots of a 100 mM ZnSO₄ stock solution increased the total concentration of zinc in the solution. The volume of zinc added never exceeded 5% of the total volume. Isotherms were fit as previously reported³ using Igor Pro.

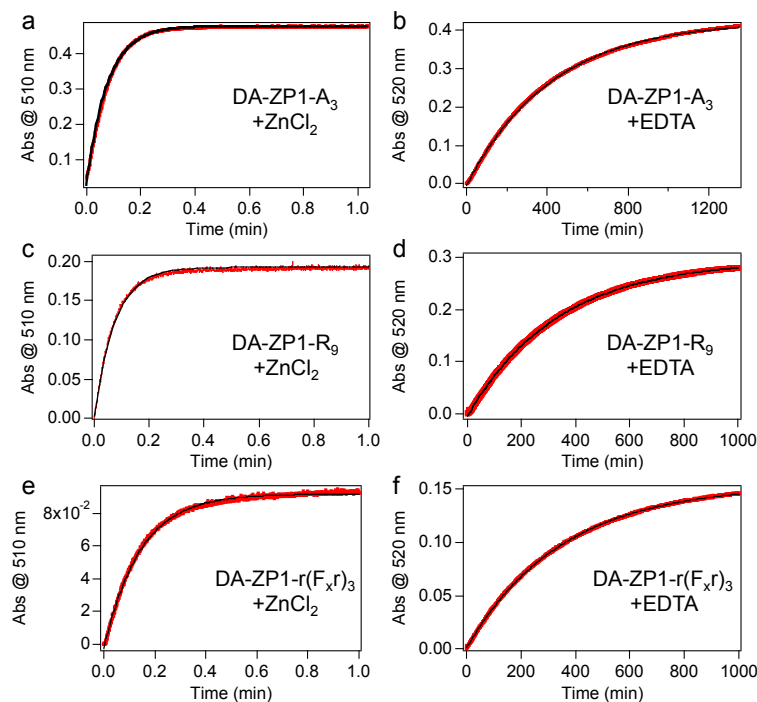


Figure S7. Representative kinetic traces (red dots) and fits (black line) for deacetylation of DA-ZP1-peptides in buffer at 37 °C. DA-ZP1-A₃ (5.5 μM) with (a) 100 μM ZnCl₂ or (b) 100 μM EDTA. DA-ZP1-R₉ (2 μM) with (c) 100 μM ZnCl₂ or (d) 100 μM EDTA. DA-ZP1-r(F_xr)₃ (1 μM) with (e) 100 μM ZnCl₂ or (f) 100 μM EDTA. Data were fit to a single exponential function using Igor Pro software. Calculated k_{obs} and $t_{1/2}$ are listed in Table S2.

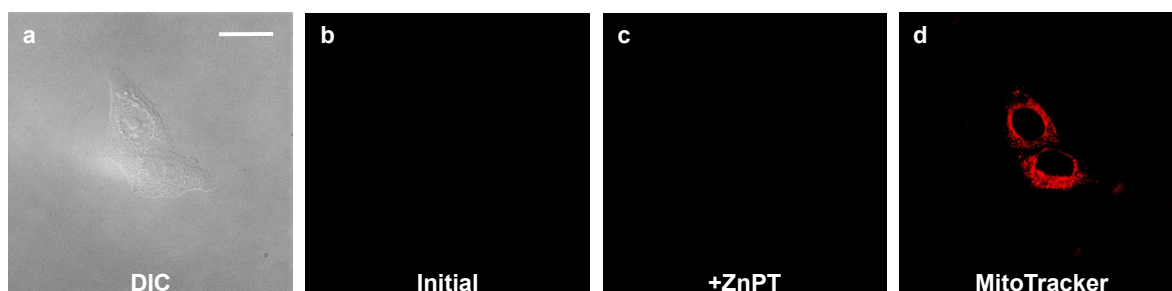


Figure S8. Live cell images of HeLa cells pretreated with 2.5 μM DA-ZP1-R₉ and 250 nM MitoTracker Red for 30 min at 4 °C. (a) DIC image. No significant signal from DA-ZP1-R₉ is observed (b) initially or (c) after addition of 25 μM ZnPT. (d) Signal from MitoTracker Red.

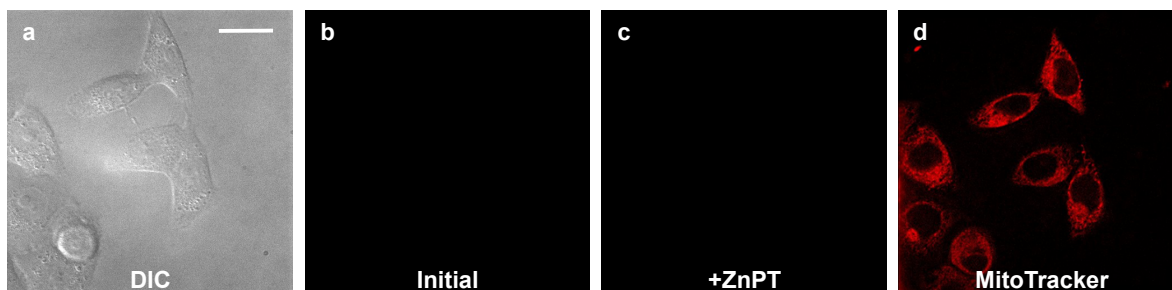


Figure S9. Live cell images of HeLa cells pretreated with 2.5 μM DA-ZP1-r(F_xr)₃ and 250 nM MitoTracker Red for 30 min at 4 °C. (a) DIC image. No significant signal from DA-ZP1-r(F_xr)₃ is observed (b) initially or (c) after addition of 25 μM ZnPT. (d) Signal from MitoTracker Red.

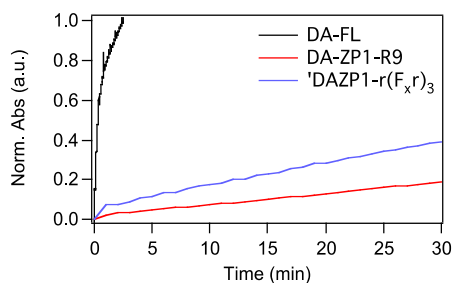


Figure S10. Increase in normalized absorbance for solutions of fluorescein diacetate (DA-FL, black line), DA-ZP1-R₉ (red line), or DA-ZP1-r(F_xr)₃ (blue line) in buffer (50 mM PIPES, 100 mM KCl; pH 7) at 37 °C after addition of 0.25 units of porcine live esterase (Sigma).

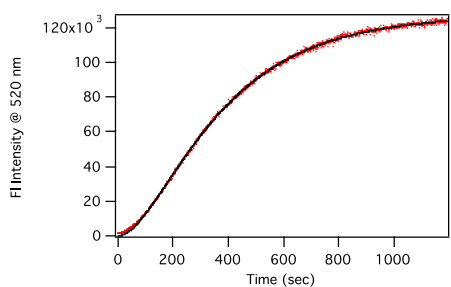


Figure S11. Data (red dots) and fit (black line) for the increase in fluorescence intensity of a solution containing 0.5 μM DA-DCF-r(F_xr)₃ in buffer (50 mM PIPES, 100 mM KCl; pH 7) at 37 °C after addition of 0.25 units of porcine live esterase (Sigma). Data were fit to two irreversible reactions using DynaFit as previously described.⁴ $k_{\text{obs-1}} = 0.0102(2) \text{ s}^{-1}$; $k_{\text{obs-2}} = 0.0041(7) \text{ s}^{-1}$.

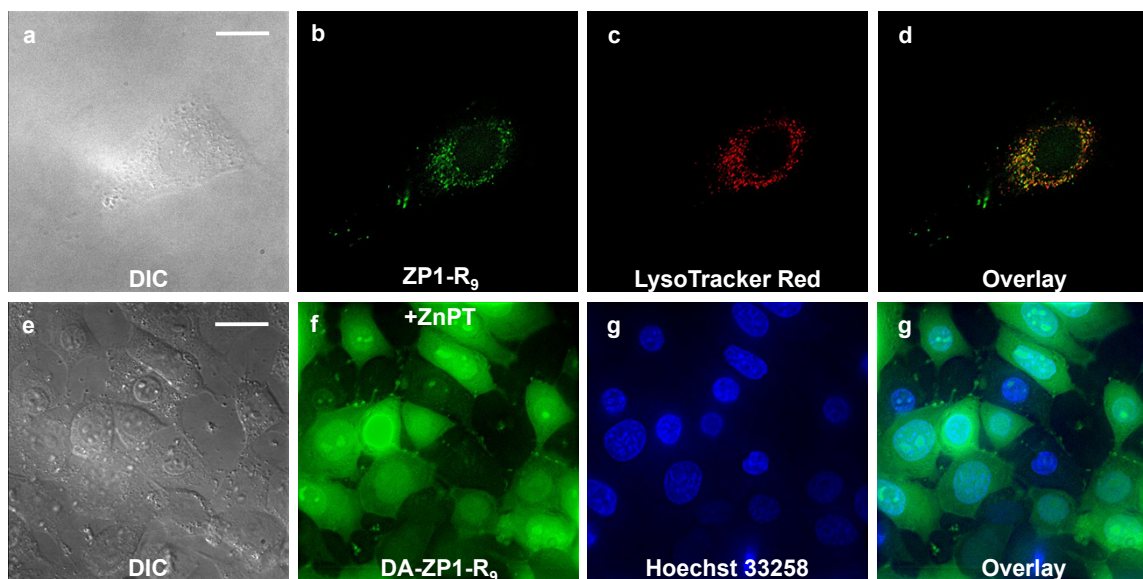


Figure S12. Full-field view of main text Fig 3. Fluorescence microscopy images of live HeLa cells pretreated with ZP1-R₉ (5 μM) or DA-ZP1-R₉ (2.5 μM) and the indicated organelle stain. Top, ZP1-R₉: (a) DIC image, (b) signal from ZP1-R₉, (c) signal from LysoTracker Red, (d) overlay of (b) and (c). Pearson's $r = 0.42 \pm 0.16$ ($n = 8$). Bottom, DA-ZP1-R₉: (e) DIC, (f) signal from DA-ZP1-R₉ after treatment with 25 μM ZnPT, (g) signal from Hoechst 33258, (h) overlay of (f) and (g). Scale bar = 25 μm

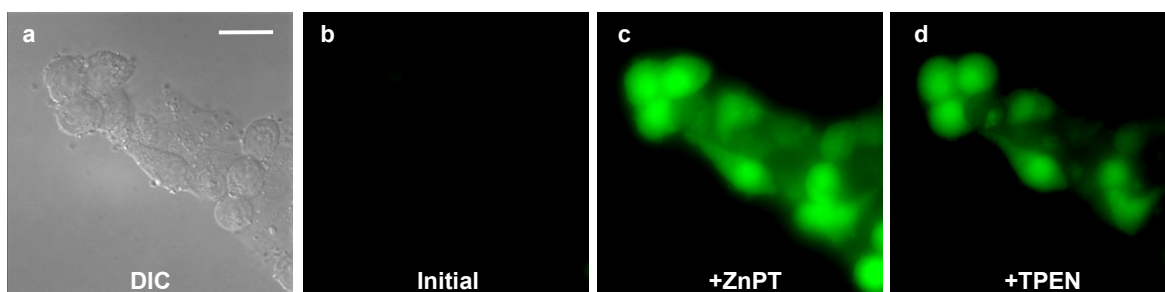


Figure S13. Full-field view of main text Fig 4. Response of DA-ZP1-R₉ to zinc pyrithione in live HeLa cells. (a) DIC image. Signal from DA-ZP1-R₉ (b) initially, (c) after addition of 25 μM ZnPT, and (d) after addition of 50 μM TPEN. Scale bar = 25 μm.

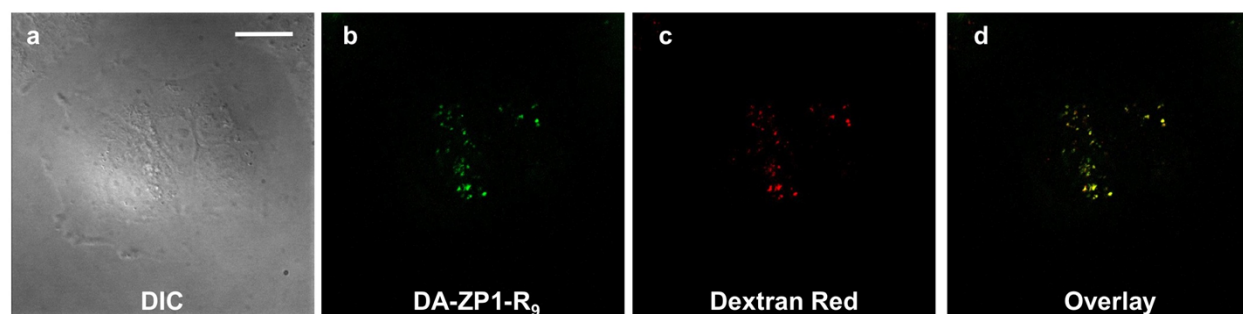


Figure S14. Full-field view of main text Fig. 5. Fluorescence microscopy of live HeLa cells pretreated with 1 μM DA-ZP1-R₉ and 100 nM Dextran Red. (a) DIC image, (b) signal from DA-ZP1-R₉ after addition of 25 μM ZnPT (c) signal from Dextran Red, (d) overlay of (b) and (c). Pearson's $r = 0.55 \pm 0.12$ ($n = 11$). Scale bar = 25 μm

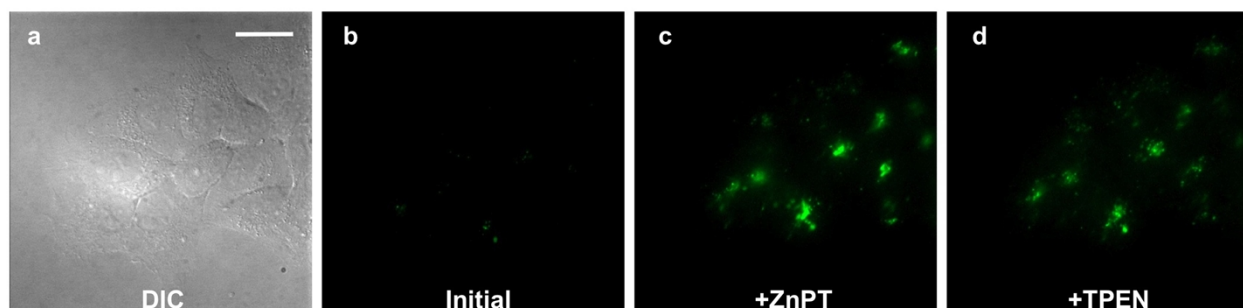


Figure S15. Full-field view of main text Fig. 6. Fluorescence microscopy of live HeLa cells pretreated with 1 μM DA-ZP1-R₉. (a) DIC image, signal from DA-ZP1-R₉ (b) initially, (c) after addition of 25 μM ZnPT, and (d) after addition of 50 μM TPEN.

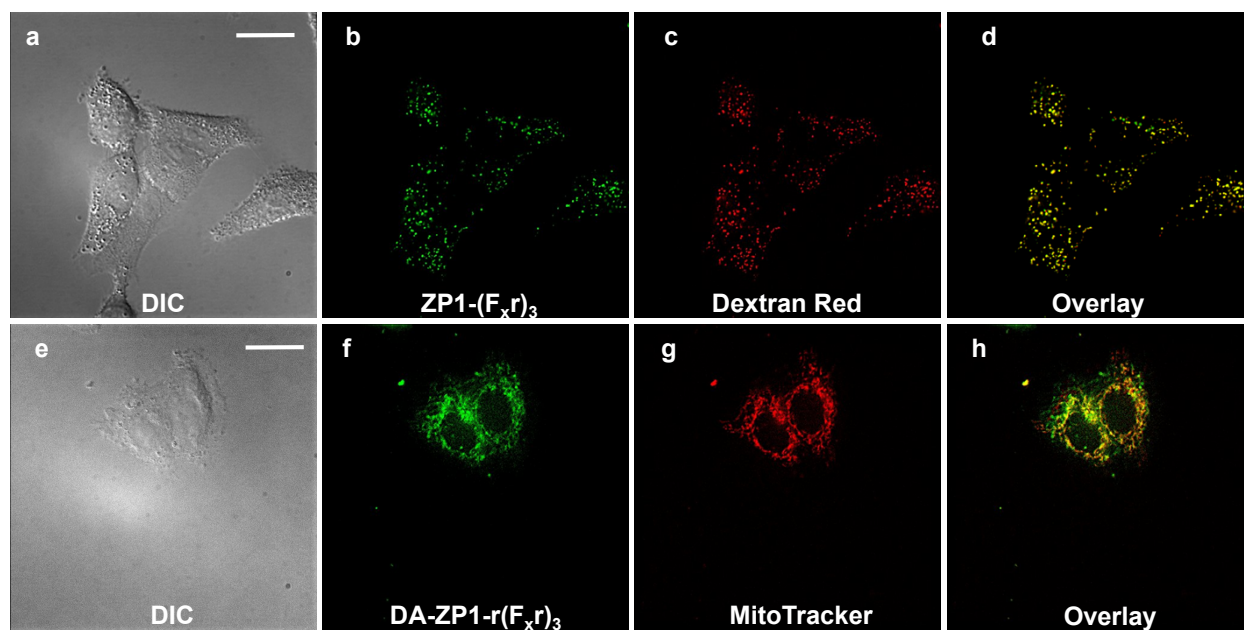


Figure S16. Full-field view of main text Fig. 7. Fluorescence microscopy of ZP1-(F_{x,r})₃ and DA-ZP1-r(F_{x,r})₃ in live HeLa cells. Top, cells pretreated with medium containing 2.5 μM of ZP1-(F_{x,r})₃: (a) DIC image, (b) signal from ZP1-(F_{x,r})₃, (c) signal from Dextran Red, (d) overlay of (b) and (c). Pearson's $r = 0.71 \pm 0.07$. Bottom, cells pretreated with 1 μM DA-ZP1-r(F_{x,r})₃: (e) DIC, (f) signal from DA-ZP1-r(F_{x,r})₃ after treatment with 25 μM ZnPT, (g) signal from MitoTracker Red, (h) overlay of (f) and (g). Pearson's $r = 0.41 \pm 0.09$. Scale bar = 25 μm

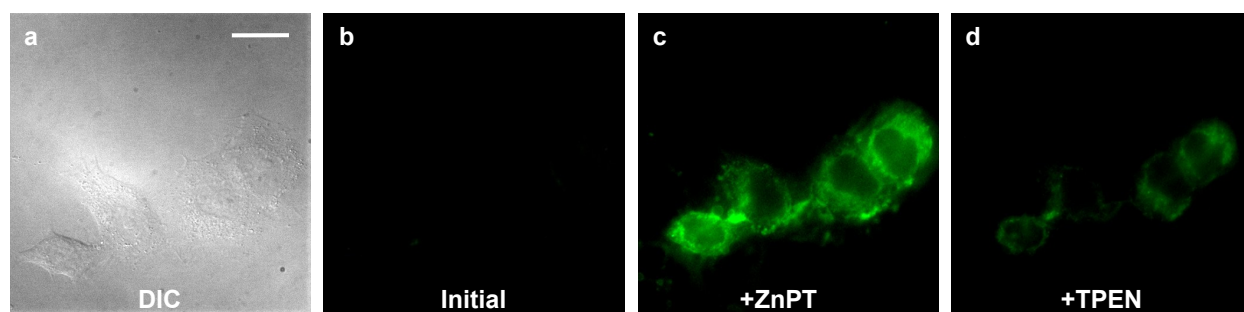


Figure S17. Full-field view of main text Fig. 8. Response of DA-ZP1-r(F_{x,r})₃ to zinc pyrithione in live HeLa cells. (a) DIC image. Signal from ZP1-r(F_{x,r})₃ (b) initially, (c) after addition 25 μM ZnPT, and (d) after addition of 50 μM TPEN. Scale bar = 25 μm

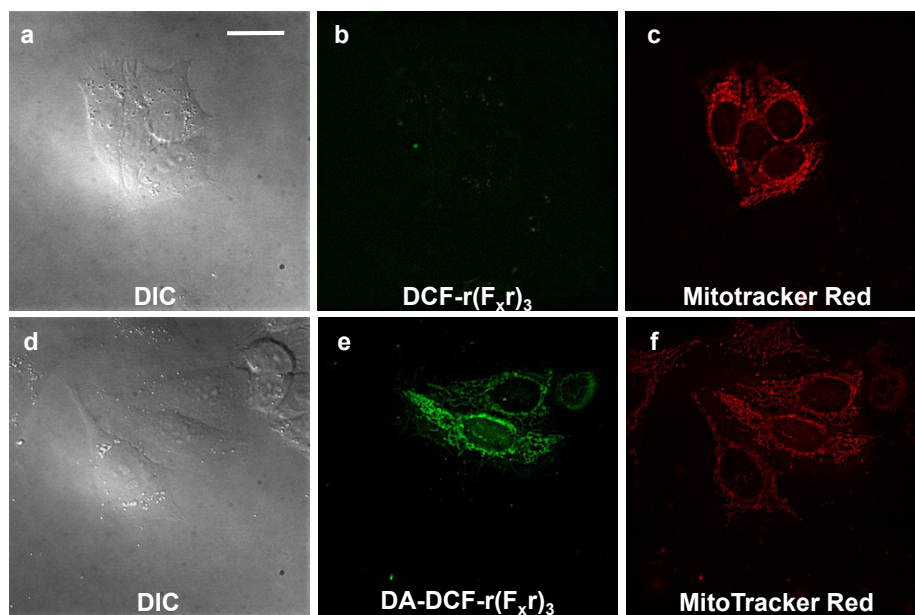


Figure S18. Full-field view of main text Fig. 9. Fluorescence microscopy of DCF-(F_{xr})₃ and DA-DCF-r(F_{xr})₃ in live HeLa cells. Top, cells pretreated with 5 μM DCF-r(F_{xr})₃ and 500 nM MitoTracker Red for 30 min. (a) DIC image, (b) signal from DCF-r(F_{xr})₃, (c) signal from MitoTracker Red. Bottom, cells pretreated with 5 μM DA-DCF-r(F_{xr})₃ and 500 nM MitoTracker Red for 30 min. (d) DIC, (e) signal from DCF-r(F_{xr})₃, (f) signal from MitoTracker Red. The global Pearson's r is 0.57 ± 0.16 ($n = 37$). Cells with high levels of DA-DCF-r(F_{xr})₃ (e, red outline) have a higher Pearson's $r = 0.83 \pm 0.08$ ($n = 10$). Scale bar = 25 μm

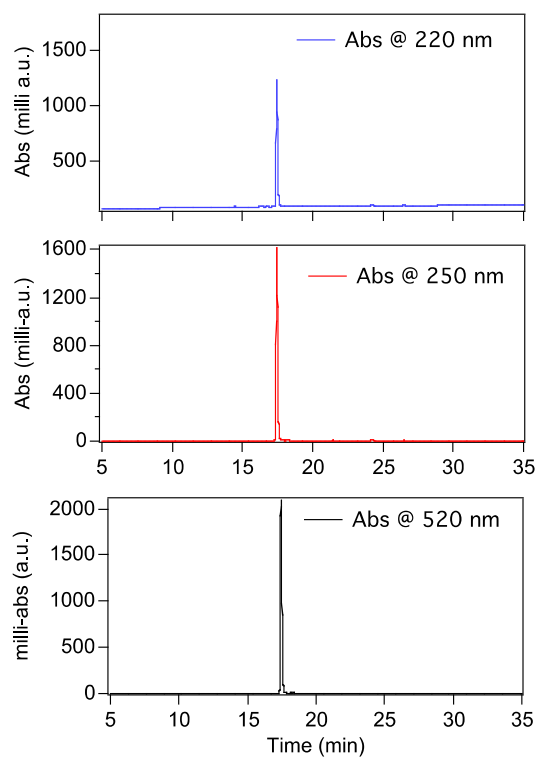


Figure S19. Analytical HPLC chromatogram for ZP1-A₃.

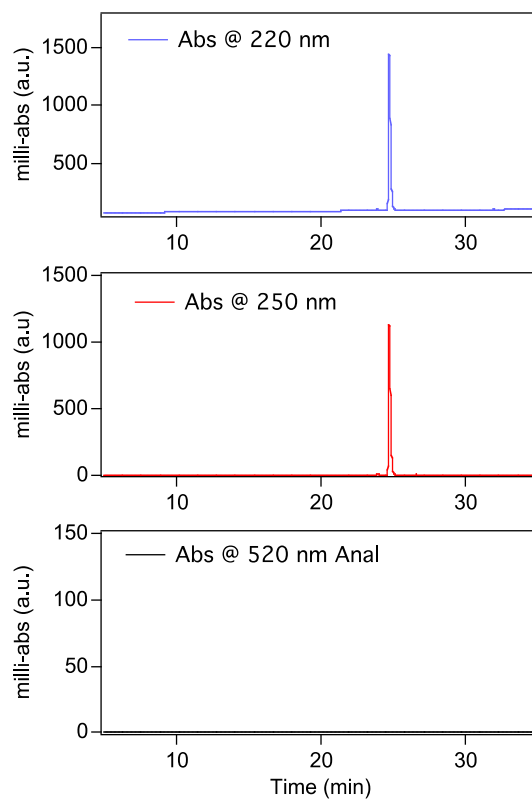


Figure S20. Analytical HPLC chromatogram for DA-ZP1-A₃.

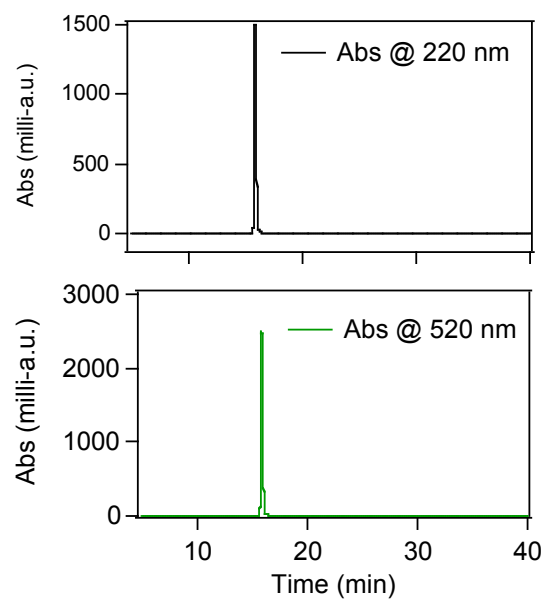


Figure S21. Analytical HPLC chromatogram for ZP1-R₉.

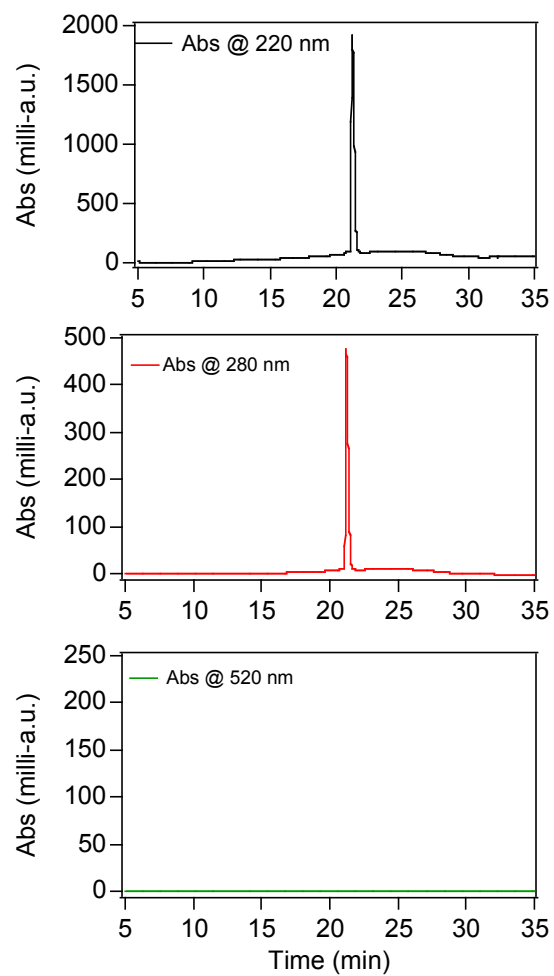


Figure S22. Analytical HPLC chromatogram for DA-ZP1-R₉.

Figure S23. Analytical HPLC chromatogram for ZP1-(F_xr)₃.

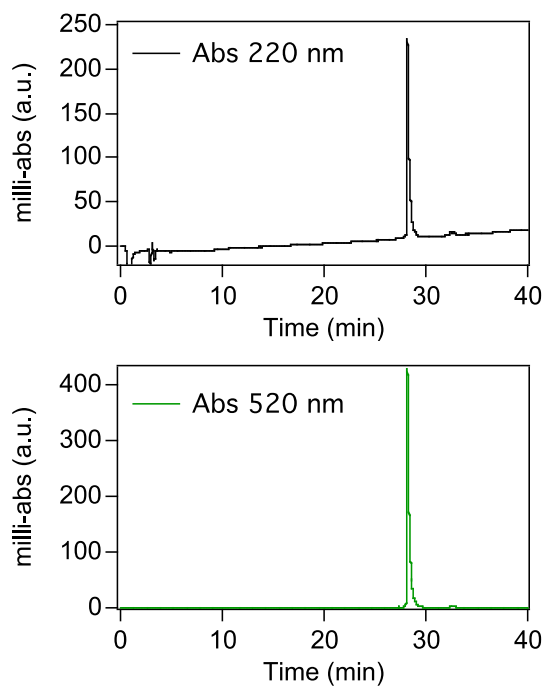
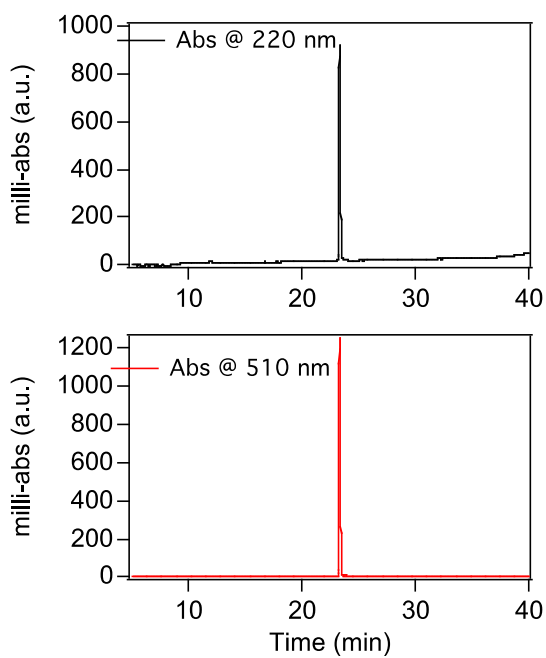


Figure S24. Analytical HPLC chromatogram for ZP1-r(F_xT)₃.



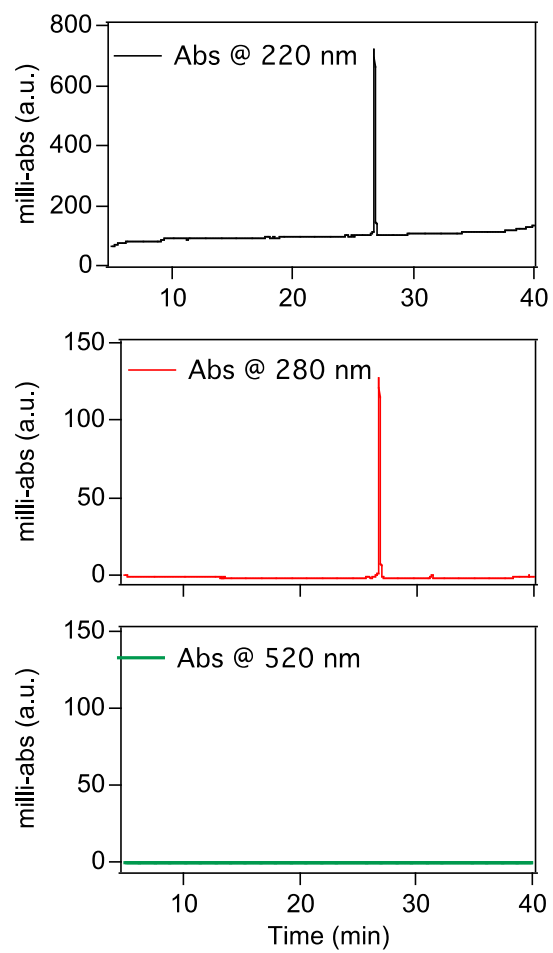


Figure S25. Analytical HPLC chromatogram for DA-ZP1-r(F_xr)₃.

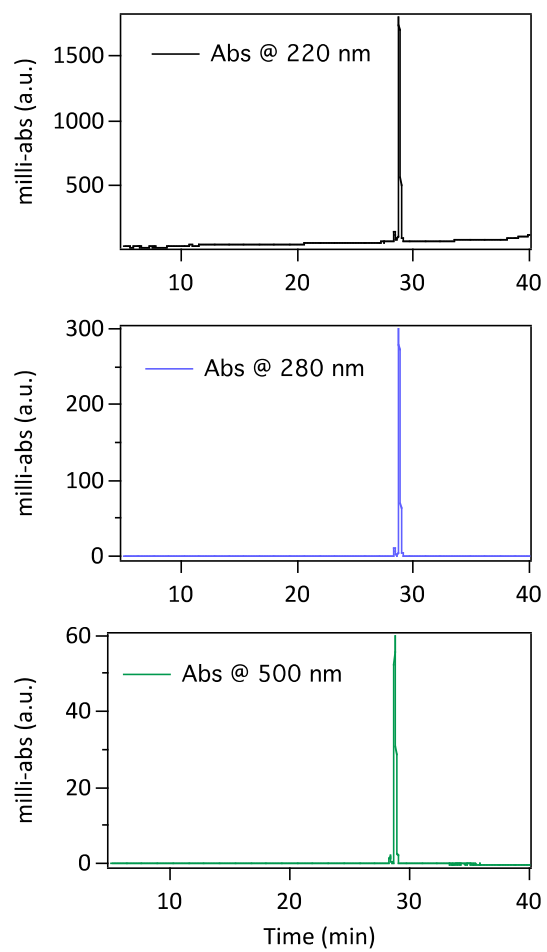


Figure S26. Analytical HPLC chromatogram of DCF-r(F_xT)₃.

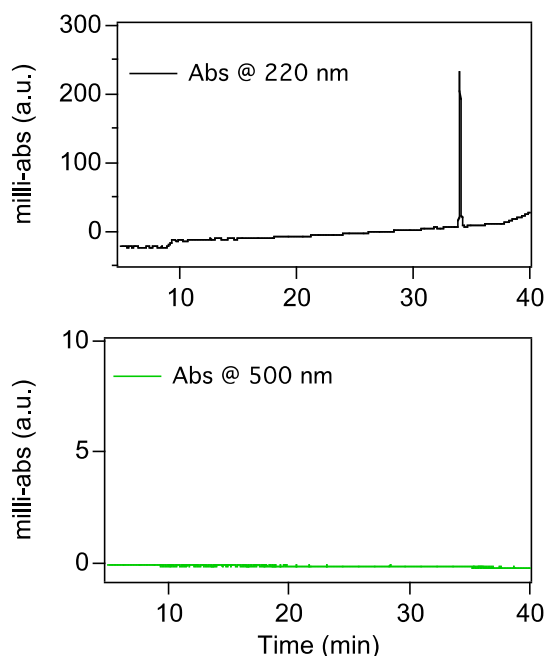


Figure S27. Analytical HPLC chromatogram of DA-DCF-r(F_{xR})₃.

References

1. C. C. Woodroffe, R. Masalha, K. R. Barnes, C. J. Frederickson and S. J. Lippard, *Chem. Biol.*, 2004, **11**, 1659-1666.
2. (a) S. I. Kirin, F. Noor, N. Metzler-Nolte and W. Mier, *J. Chem. Educ.*, 2007, **84**, 108-111; (b) R. J. Radford, W. Chyan and S. J. Lippard, *Chem. Sci.*, 2013, **4**, 3080-3084.
3. G. K. Walkup, S. C. Burdette, S. J. Lippard and R. Y. Tsien, *J. Am. Chem. Soc.*, 2000, **122**, 5644-5645.
4. W. Chyan, D. Y. Zhang, S. J. Lippard and R. J. Radford, *Proc. Natl. Acad. Sci. USA*, 2014, **111**, 143-148.
5. A. P. French, S. Mills, R. Swarup, M. J. Bennett and T. P. Pridmore, *Nat. Protoc.*, 2008, **3**, 619-628.
6. E. M. Nolan and S. J. Lippard, *Acc. Chem. Res.*, 2009, **42**, 193-203.